P3.4 SOME RESULTS FROM A SOUNDING ENHANCED OBSERVING PERIOD FOCUSED ON LOW CEILING AND VISIBILITY IN THE NORTHEASTERN UNITED STATES

Robert Tardif *

National Center for Atmospheric Research, Research Applications Laboratory, Boulder, Colorado

1. INTRODUCTION

This paper reports on activities performed in the context of improving our understanding of the various mechanisms influencing the life cycle of low ceiling and visibility (C&V) conditions in a complex area. From a geographical point of view, the focus is on an area around New York City (NYC) in the northeastern (NE) United States. The area offers a wide variety of scenarios leading to low C&V conditions (Tardif 2004) and thus represents a suitable location for the study of varied C&V regimes. Also, efforts are underway toward the development of tools aimed at improving C&V forecasts on a national scale (Herzegh et al 2006) as well as for the major terminals in the NYC area (Clark 2006, Robasky and Wilson, 2006). Therefore an increased understanding of the physical mechanisms leading to low C&V occurrences can support these initiatives.

A component of the overall efforts is the analysis of observations gathered from a field site located at the Brookhaven National Laboratory in eastern Long Island NY (Tardif et al. 2004). A preliminary analysis of observations from the field site during low C&V conditions has led to hypothesize about the important role of processes occurring aloft in influencing the evolution of low C&V conditions. Therefore, an Enhanced Observing Period (EOP) was performed in May 2005 during which the NCAR mobile GPS LORAN Sounding System (GLASS) was deployed at the C&V field site. The objective was the sampling of the vertical structure of the lower atmosphere during variable C&V conditions to determine to which extent changes in C&V conditions are influenced by changes in the atmospheric structure aloft.

A climatological analysis of low C&V events has shown that May is the month during which such events are most likely in the area. Unfortunately, the number of low C&V events that took place during the EOP proved to be below the climatological frequency. In fact, no fog events occurred during the EOP. Nevertheless, rawinsondes were launched during a total of five low ceiling events, complementing the routine soundings performed at the nearby National Weather Service office in Upton NY. Case study analyses of two of the events are presented here, highlighting the observations of the evolution of the atmosphere's vertical structure, as well as other relevant features associated with events difficult to forecast accurately. Results are presented showing the mechanisms leading to the inland intrusion of marine stratus, as well as features associated with the nighttime dissipation of another low cloud system.

* *Corresponding author address*: Robert Tardif, NCAR-RAL, PO Box 3000, Boulder, CO, 80307. E-Mail: tardif@ucar.edu

2. SITE LOCATION AND DATA

The sounding EOP was performed at an instrumented site located on the campus of the Brookhaven National Laboratory (BNL) in east-central Long Island, NY (Fig. 1). The NCAR mobile GLASS consists of a vehicle fitted with equipment used to launch and track weather balloons as well as with surface sensors measuring ambient temperature, humidity and wind. During the EOP, balloons were configured for slow ascent in order to maximize the number of data points in the boundary layer. Biases in temperature and humidity from the Vaisala RS-80 sondes were corrected using comparisons with concurrent surface observations from the mobile GLASS and from an instrumented tower.

Complementing the rawinsondes, the observational capabilities include a Vaisala laser ceilometer and a 90-m instrumented tower. The tower is instrumented with three visibility/present weather sensors at the base, middle and top of the tower, 7 levels of temperature, humidity and wind measurements, two shortwave and longwave radiometers providing measurements of upwelling and downwelling radiation and two sets of fast response temperature and humidity flux measurement systems. Surface instruments include an additional set of temperature/relative humidity sensors at 2 m, a barometric pressure probe and a GEONOR precipitation gauge. Soil temperature and moisture are measured at the site at five levels. Remote sensing capabilities include a 12-channel profiling microwave radiometer providing retrievals of temperature and humidity profiles as well as cloud water content (Ware et al., 2003).

Other available data include 1-min surface measurements obtained from the network of Automated Surface Observing System (ASOS). Hourly data from buoys located in the coastal waters around Long Island are also available through NOAA's National Data Buoy Center. See Fig. 1 for the location of the ASOS sites and buoys. Furthermore, GOES-12 satellite imagery and derived products such as the fog product from NOAA's National Environmental Satellite Data and Information Service (NESDIS) using the bi-spectral technique of Ellrod (1995), as well as the Navy Research Laboratory (NRL) cloud classification product (Bankert and Hawkins 2003), are used to track low cloud systems.

Figure 1. Location of the instrumented C&V site (red square and arrow), main ASOS sites (white dots) and buoys (blue dots. The location of a coastal rawinsonde launch (Smith Point) is indicated by the green dot.

Furthermore, hourly analyses from the Rapid Update Cycle (RUC) (Benjamin et al 2004) at 13 km resolution are used to characterize the evolving mesoscale flow environment as well as the spatial variability of temperature and moisture over the coastal region.

3. CASE STUDIES

During the period from May 2nd to May 26th, constant monitoring of weather conditions and forecasts were used to determine the pertinence of launching rawinsondes during low C&V events in order to obtain measurements of conditions aloft pertaining to the evolution of C&V conditions. Salient features observed during some of the events are discussed in the form of case study analyses and main findings are summarized.

3.1 Marine stratus intrusion

A low ceiling event occurred over Long Island, southern New Jersey, southern New York State and southern Connecticut during the mid to late night hours on May 11th 2005. This event resulted from an unforeseen northward propagation of a marine stratus cloud system over the coastal land areas. The life cycle of this event is described and analyzed using routine and research weather observations.

On the late afternoon hours on the 10th, the stratus was well offshore south of Long Island but hugging the coast of the Delmarva Peninsula and southern New Jersey (Fig. 2). The marine cloud retreated southward for most of the day on the 10th under the influence of boundary layer flow with a northerly component driven by the large scale pressure gradient found between a low pressure system centered well offshore of the mid-Atlantic states and a high pressure system over the coastal areas of New Jersey and Delmarva Peninsula (Fig. 3). Observations at coastal stations along Long Island and New Jersey (Fig. 4) indicate the presence of an onshore flow due to a sea-breeze circulation in the immediate vicinity of the coast.

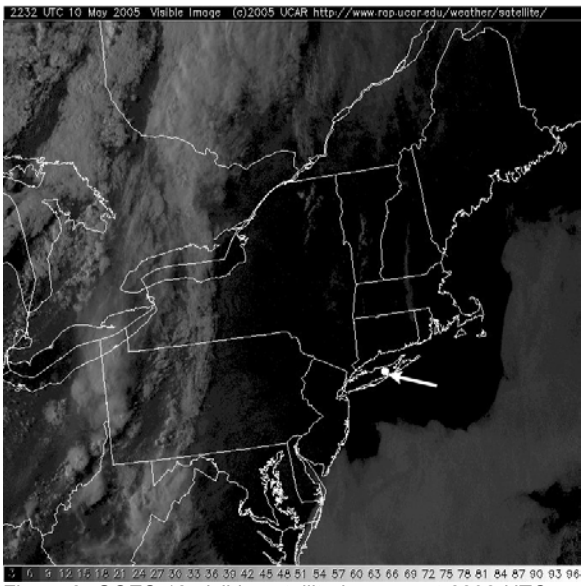

Figure 2. GOES-12 visible satellite imagery at 2232 UTC on May 10th 2005. The arrow indicates the location of the EOP site.

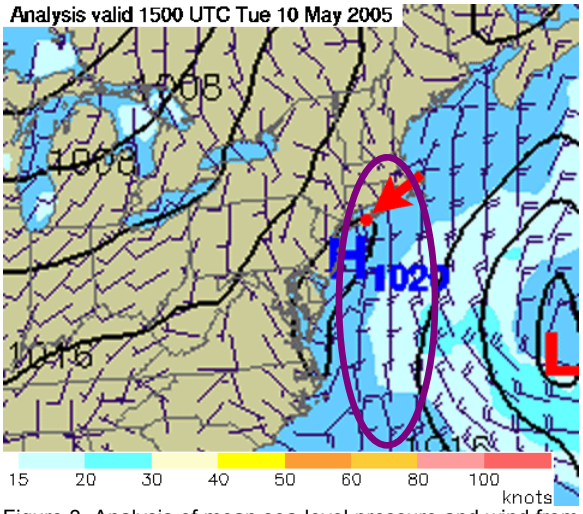

Figure 3. Analysis of mean sea-level pressure and wind from the RUC, at 1500 UTC on May 10th 2005. The red arrow and dot indicate the location of the EOP site.

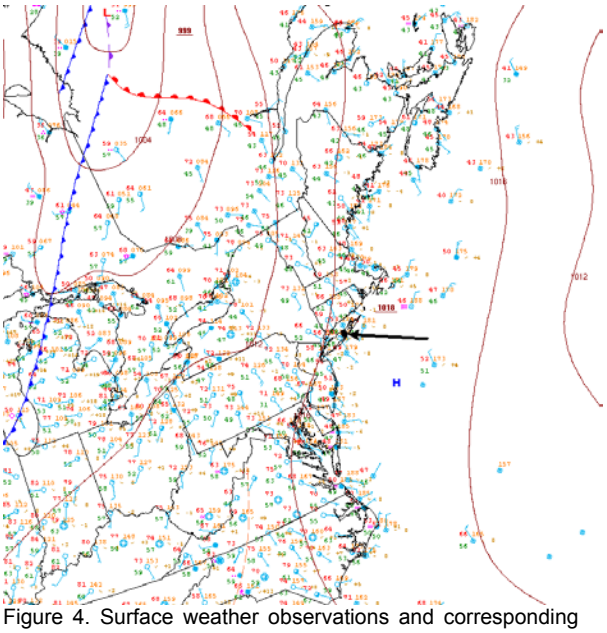

Figure 4. Surface weather observations and corresponding sea-level pressure and frontal analyses from the NWS Hydrometeorological Prediction Center, at 0000 UTC on May 11th 2005. The arrow indicates the location of the EOP site.

The 00 UTC sounding at Upton NY (OKX) shows further evidence of the penetration of a sea breeze. The temperature profile shows a 250-m deep cooler layer associated with a light onshore breeze (flow from the SSW) (Fig. 5). The wind speed in fact was decreasing in the BL and rapidly veered to W with speeds of about 2 to 3 m s^{-1} above. A strong inversion was located at the top of the layer in which the intrusion of the marine air took place.

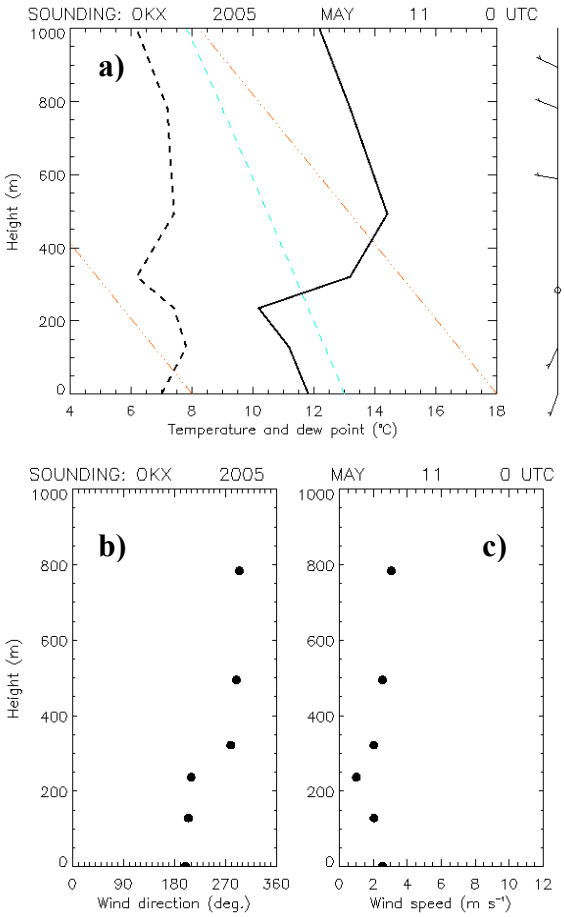

Figure 5. Profiles of a) temperature (solid line) and dew point temperature (dashed line), b) wind direction and c) wind speed from 00 UTC OKX sounding on May 11th 2005. The light blue dashed line in (a) represents a moist-adiabatic lapse rate, while the dot-dashed orange line represents a dry adiabatic lapse rate.

Images from NRL's nighttime cloud classification product (Bankert and Hawkins 2004) provide evidence of the northward propagation of the marine stratus cloud system during the first half of the night on the 11th (Fig. 6). In fact, a relatively narrow tongue of stratus propagated northward faster at longitudes corresponding to middle and eastern Long Island compared to adjacent areas. High-resolution satellite imagery focused on the NYC area confirms the presence of an approaching low cloud just offshore of Long Island at 0300 UTC (Fig. 7). Observations from the ceilometer indicate that the stratus reached the field site at 0330 UTC with a cloud base at about 150 m (Fig. 8).

The first rawinsonde released after the arrival of the cloud shows a typical vertical structure of cloud-topped boundary layers. The temperature lapse rate in the subcloud layer is equal to the dry adiabatic lapse rate and is moist-adiabatic within the cloud layer (Fig. 9a). This is indicative of a well-mixed cloud-

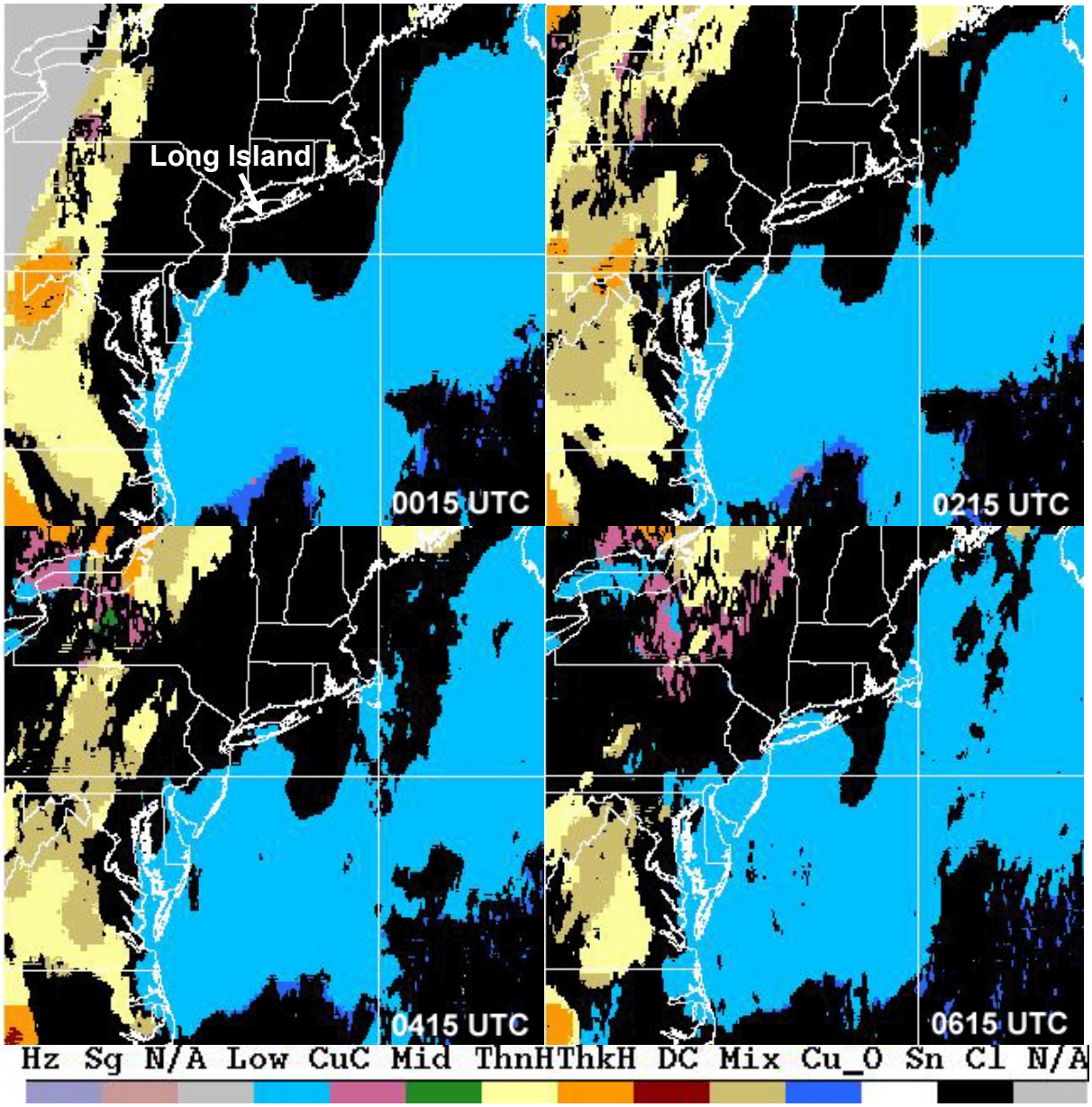

Figure 6. Images depicting the evolution of the marine stratus cloud over the coastal waters off the coast of the Delmarva Peninsula, New Jersey and south of Long Island, from 0015 UTC to 0615 UTC on May 11th 2005. Images are from NRL's nighttime cloud classification product. As the legend at the bottom of the figure indicates, the light blue areas indicate the presence of a low cloud deck.

topped boundary layer with a cloud layer fully coupled to the surface layer. A strong inversion is found to originate near cloud top, with a change in temperature of 5°C over a layer 150 m deep above the cloud. In contrast to typical conditions found in the subsidence regions of the eastern Pacific during summer, the moisture above the cloud layer does not decrease dramatically. In terms of the wind profile, the flow was from the SSW below the cloud, turning to the S in the cloud layer and transitioning to a flow from the SW above the cloud (Fig. 9b). This transition took place over a shallow layer, between 375 m and 425 m in height. The wind speed increased with height in the boundary layer, reaching a maximum of 8.5 m s^{-1} at the top of the cloud layer (Fig 9c). A comparison with the 00 UTC OKX sounding (Fig. 5) shows that a substantial acceleration of the flow occurred at the top of the boundary layer during the night. In fact, the speed of the wind observed at the top of the cloud at 0547 UTC corresponds to the speed at which the cloud propagated northward (deduced from the sequence of satellite imagery).

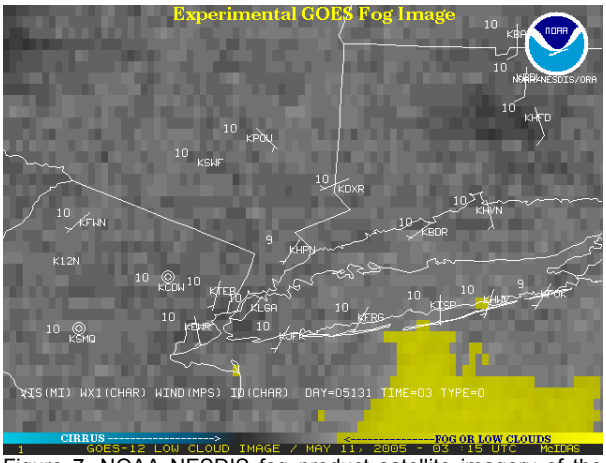

Figure 7. NOAA NESDIS fog product satellite imagery of the New York area on 03 UTC May 11th 2005.

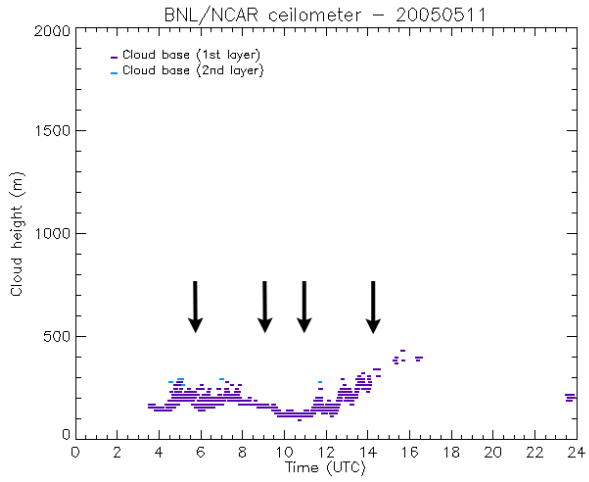

Figure 8. Temporal evolution of ceilometer observations of cloud base heights at the FAA C&V field site on May 11th 2005. Arrows indicate times at which rawindsondes were launched.

Therefore, the key elements that led to this low ceiling event over terminals in the New York area correspond to the mechanisms that generated the low-level flow conditions and the environmental characteristics of the lower atmosphere that allowed the cloud layer to persist as it propagated northward.

As presented previously, the presence of a ridge over the coastal areas of the northeastern United States provided for weak pressure gradients over the coastal areas south of Long Island (Fig. 5). However, the surface analyses from the RUC at a resolution of 13 km (RUC13) reveal the presence of a persistent anticyclonic mesoscale vortex centered offshore (Fig. 10). The mesoscale anticyclonic circulation is likely the result of the interaction of thermally-induced sea breezes over the coastal zones of Long Island and New Jersey, as well as the circulation associated with the high pressure center located just offshore of the Delmarva peninsula. The enhanced southerly return circulation within the boundary layer on the western edge of this vortex corresponds to the region where the stratus cloud propagated northward over the coastal Atlantic during the early evening hours. Also noticeable is the southeasterly flow over the coast in southern New Jersey, corresponding well to the inland propagation of the low clouds in that region. Therefore a good agreement is found between the wind field from the RUC13 analyses and the observed propagation of the marine stratus. Nevertheless, the wind speed at the top of the boundary layer is underestimated by several m s^{-1} in the RUC analyses compared to the available sounding data. Despite this underestimation, the results suggest the circulation associated with the mesoscale vortex seem to have played a central role in bringing the cool, moist and cloudy marine boundary layer air over the coastal areas of Long Island and New Jersey.

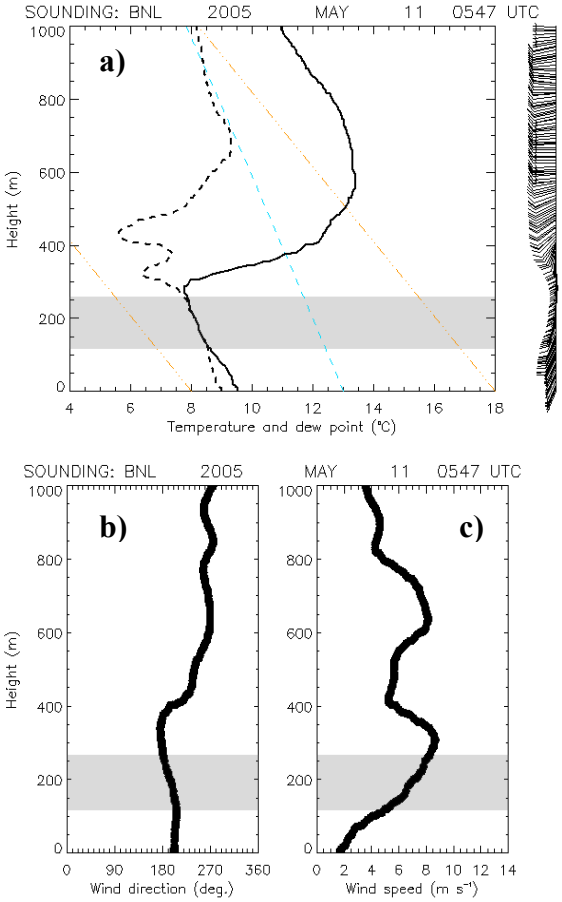

Figure 9. Same as Fig. 7 but with data from a GLASS sounding launched at the BNL tower site at 0547 UTC on May 11th 2005. Gray shared areas indicate the estimated location of the cloud layer.

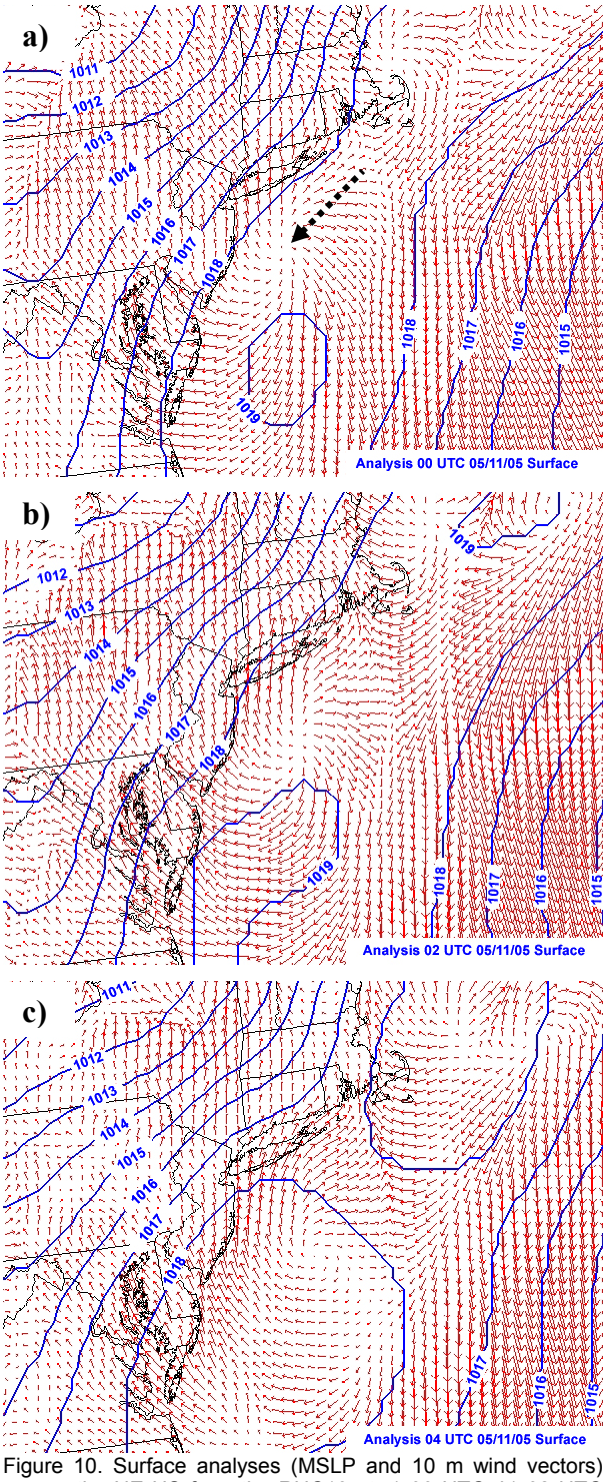

Figure 10. Surface analyses (MSLP and 10 m wind vectors) over the NE US from the RUC13 at a) 00 UTC, b) 02 UTC and c) 04 UTC on May 11th 2005. The center of an anticyclonic vortex is indicated by a dashed arrow in the top figure.

Often quoted as important factors in the forecasting of low ceiling conditions are the wind shear conditions at cloud top and the moisture above the cloud. Significant wind shear across the cloud top interface and the presence of a dry enough layer above cloud top enhances the entrainment of dry air within the cloud, possibly leading to buoyancy reversal of cloudy air parcels through further cooling of the air by the evaporation of the surrounding cloud drops (Siems et al. 1990). This process has been described as possibly leading to the rapid breakup of stratiform cloud layers.

Here, conditions near cloud top are examined using data from the sounding launched at 0547 UTC. A closer examination of the temperature and dew point profiles near cloud top (Fig. 11) indicates the upper level at which saturation is measured is at about 260 m. This is likely to top of the completely cloudy layer. Above that layer, the humidity sensor showed a slight departure from saturation over a layer of 25 m in depth while the temperature lapse rate remains close to the moist-adiabatic. Another transitional layer is observed above (from 285 m to 305 m) in which the relative humidity indicates a greater departure from saturation and the temperature profile shows a transition to a statically stable lapse rate.

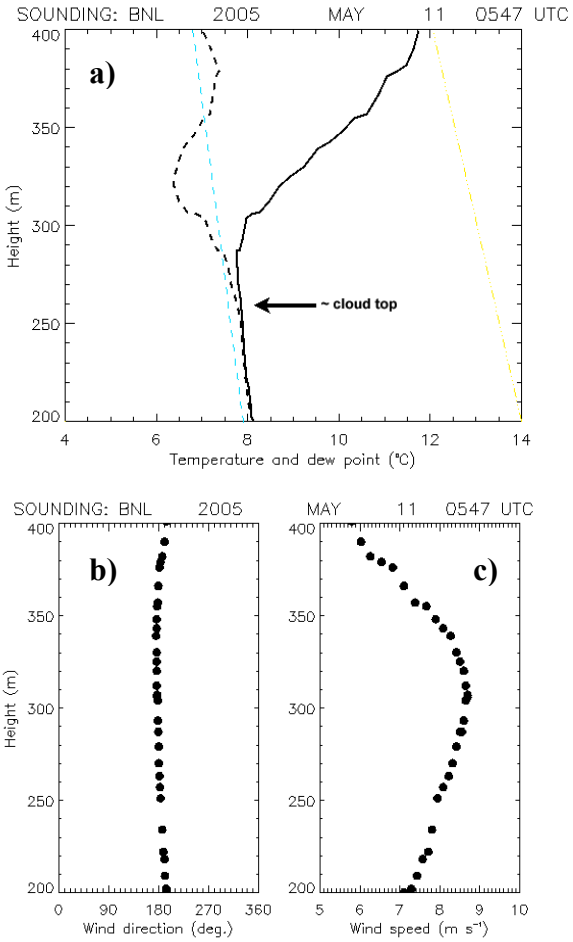

Figure 11. Same as Fig. 8, but zoomed on conditions around cloud top.

This layer is superimposed by the main inversion, in which the largest vertical gradients in temperature and humidity are found. The observed fine-scale structure at cloud top is consistent with the study by Moeng et al. (2005) who found that the cloud top is generally located below the main inversion by a few tens of meters.

The conditions of turbulence and entrainment near cloud top are examined as they relate to the likelihood of its breakup versus its persistence as it advected inland. First, the profile of specific humidity indicates that the lower free atmosphere was quite humid (Fig. 12). Apart from slight variations just above cloud top, specific humidity values in the lower free troposphere were slightly larger than within the well-mixed boundary layer. To assess the likelihood of turbulent mixing above cloud top, the Richardson number is calculated using observations of virtual potential temperature (θ_v) and wind components (u, v):

$$R_i = \frac{g}{\overline{\theta_v}} \frac{\dfrac{\partial \overline{\theta_v}}{\partial z}}{\left[\left(\dfrac{\partial u}{\partial z}\right)^2 + \left(\dfrac{\partial v}{\partial z}\right)^2\right]} \qquad (1)$$

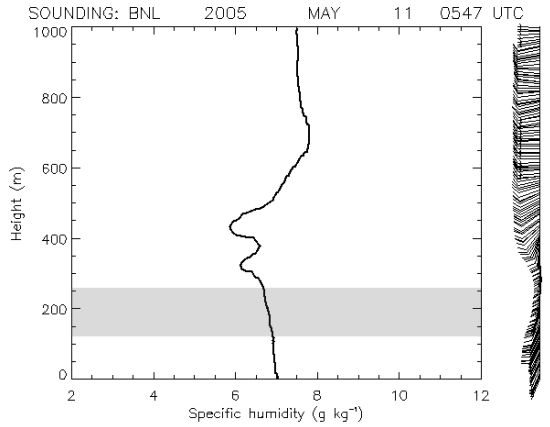

Figure 12. Profile of the specific humidity derived from data from the GLASS sounding launched at the BNL tower site at 0547 UTC on May 11th 2005. Gray shared areas indicate the estimated location of the cloud layer.

The wind shear in the vicinity of cloud top is estimated to be of the order of 1.5 m s^{-1}/100m, without significant directional shear (Fig. 11c). With values extracted from the sounding (Table I), a value of R_i ~ 1.5 is found for the layer just above the estimated cloud top (260m to 285m), while a value of R_i ~ 27.6 is found in the layer between 285 m and 305 m and R_i ~ 120.5 for the layer between 305 m and 325 m. Since values of R_i > 0.25 indicate non-turbulent regions, it is therefore concluded that turbulent mixing above cloud top is unlikely in this case, except perhaps in the immediate vicinity of cloud top.

Table I. Values used in the computation of R_i, extracted from observed profiles at 0547 UTC May 11th 2005.

Height	θ_v (K)	Wind speed (m s^{-1})	Wind direction
265 m	283.4	8.2	182°
285 m	283.6	8.5	180°
305 m	284.0	8.6	179°
325 m	285.4	8.5	178°

To further add to the evidence of the presence of environmental conditions conducive to the persistence of the stratus cloud layer, the cloud-top entrainment instability criterion is investigated. A cloud layer is said to be unstable under the theory of cloud-top entrainment instability (CTEI) when the following condition is met (Stevens et al. 2003):

$$\kappa \equiv \left(1 + \frac{\Delta s_l}{L \Delta q_t}\right) > \kappa_*, \qquad (2)$$

where s_l is the liquid water static energy

$$s_l = T c_p + g z - L q_l, \qquad (3)$$

with T the ambient temperature, g the gravitational acceleration, z the height above ground, L the latent heat of vaporization and q_l the liquid water content. q_t is the total amount of water (vapor + liquid). Since no direct measurement of q_l is available, it is taken as the adiabatic liquid water content estimated from cloud base and cloud top heights, as well as the observed temperature and water vapor specific humidity at cloud base. A value of $\kappa_* \approx 0.23$ is typical (Lock and McVean 1999, Stevens et al. 2003). Finite differences in equation (2) are meant to represent the contrast between conditions in the well-mixed cloudy boundary layer and in the free troposphere above. As suggested by the previous analysis on the likelihood to turbulence above cloud top, any turbulent exchanges between the cloud layer and the layer above, if any, is likely to be confined to a shallow layer just above cloud top. Therefore, finite differences are evaluated using values at cloud top and values characteristic of the layer between 285 m and 305 m. Values of $\Delta s_l \approx 1117$ J kg^{-1} and $\Delta q_t \approx$ -0.5 g kg^{-1} are found, yielding a value of $\kappa \approx 0.1$, which is smaller than κ_*. This suggests that the cloud layer was stable with respect to entrainment, meaning that air possibly entrained from just above the cloud was not dry enough to lead to significant evaporative cooling that would overcome the warming associated with the entrainment of the warm air in lower part of the inversion. Buoyancy reversal is unlikely to have occurred under such conditions. Furthermore, vertical profiles from soundings launched later during the night and early morning (Fig. 13) indicate that a

strengthening of the inversion occurred, without an appreciable drying of the lower free atmosphere. This indicates that the cloud layer remained stable with respect to the CTEI throughout the night and early morning.

In summary, the analysis of high-resolution sounding data launched during the presence of a marine stratus intrusion indicates that the environment in which the cloud propagated was such that it allowed the cloud layer to persist as it propagated northward. Only weak turbulent exchanges with the air above the cloud were to be expected, whereas the significant levels of moisture in the lower free atmosphere prevented the CTEI process to lead to the breakup of the cloud.

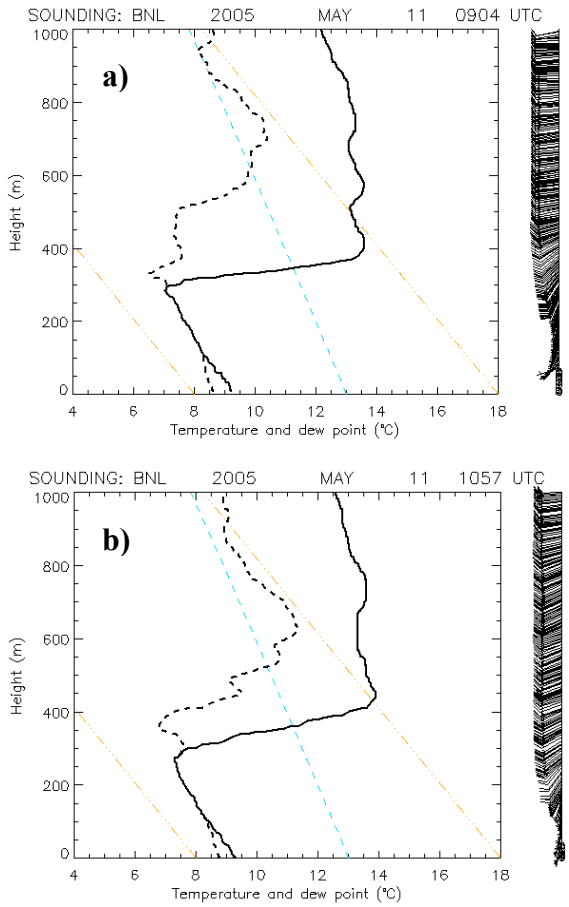

Figure 13. Same as Fig. 7 but showing data from GLASS soundings launched at the BNL tower site at a) 0904 UTC and b) 1057 UTC on May 11th 2005.

To conclude this part of the study, observations suggest that the dissipation of the cloud layer during the mid-morning hours was related to the classic "burnoff" process, whereby the increasing downwelling solar radiation transmitted though the cloud warms the surface creating unstable conditions. The turbulence in the evolving convective boundary layer warmed the layer above the dew point, leading to the dissipation of the cloud layer. The temperature and dew point profiles measured by the rawinsonde launched as the cloud had dissipated shows the presence of an unstable layer near the surface and a temperature that had warmed above the dew point throughout the depth of the boundary layer (Fig. 14).

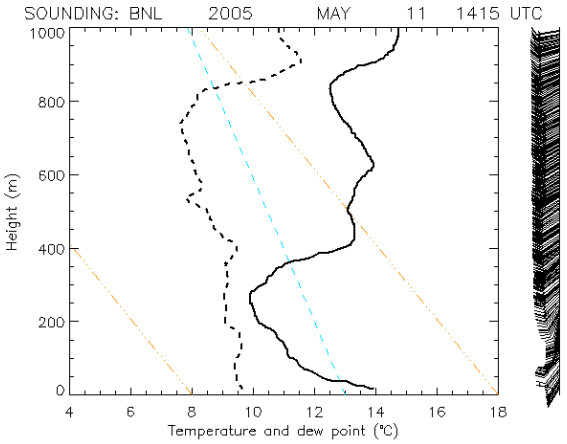

Figure 14. Same as Fig. 7 but showing data from the GLASS sounding launched at the BNL tower site at 1415 UTC on May 11th 2005.

3.2 *Nocturnal dissipation of a stratus layer*

A low ceiling event characterized by the dissipation of a stratus cloud layer one hour before sunrise occurred during the deployment of the GLASS. Rawinsondes launched during this event are analyzed to help identify the underlying mechanisms leading to cloud dissipation.

A large area of marine fog was located just offshore during the late afternoon hours on May 16th (Fig. 15). The fog began penetrating inland over coastal areas of Long Island on the early evening hours on May 17th 2005. No measures of visibility were available at the coast, but the fog was dense, with a visibility below ¼ mile (400 m). The marine cloud system propagated inland and reached the BNL tower site about 90 minutes later than first observed at the coast (Fig. 16). During its inland propagation, the marine fog transitioned into a stratus cloud layer with a base initially located at about 130 m as it reached the BNL tower site. The ceilometer data show variations in cloud base heights between 50 m and 150 m. The complete dissipation of the stratus occurred during the late night at about 0830 UTC (4:30am local time).

A comparison of profiles obtained by the sequence of soundings released before, during and after the low ceiling event provides some important information on the evolution of the vertical structure of temperature,

humidity and wind influencing the fog/stratus life cycle (Fig. 17).

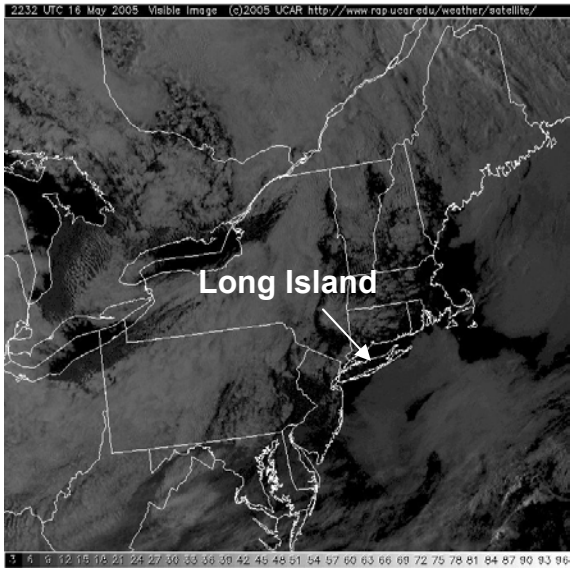

Figure 15. GOES-12 visible satellite imagery at 2232 UTC on May 16th 2005.

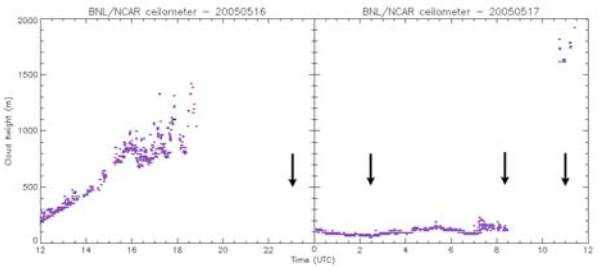

Figure 16. Ceilometer observations of cloud base heights at the BNL tower site from 12 UTC on May 16th to 12 UTC on May 17th 2005. Arrows indicate the times rawinsondes were launched.

A rawinsonde launched at the southern coast of Long Island (Smith Point, see Fig. 1) as the marine fog began its inland propagation, and at roughly the same time as the launch of the 00 UTC NWS sounding at OKX, reveals the vertical extent of the fog layer as well as the horizontal gradients between the marine environment and the boundary layer air further inland (Fig. 17a). The marine fog layer was ~100 m in depth, superimposed by a strong inversion ($\Delta T \sim +6^{o}C$ over 250 m in depth). At that time, the boundary layer air further inland was characterized by a dew point equal to the dew point of the marine air (and of the coastal SST) as a result of a sea breeze circulation that developed in the early afternoon. A difference of about $5^{o}C$ is observed between the coast and the OKX sounding location inland, as well as the vertical growth of the boundary layer up to 180 m as the marine air advected inland. This reflects the importance of surface turbulent fluxes as the marine air traveled over a warm land surface heated by solar radiation during the daytime. The sounding performed at 0231 UTC (90 minutes after the arrival of the stratus at the BNL site) shows a saturated layer up to 180 m (Fig 17b). The low level temperature became equal to the one in the marine environment upstream. This suggests that the marine cloud persisted as the marine air propagated inland only once the land surface temperature cooled to equal that of the marine air.

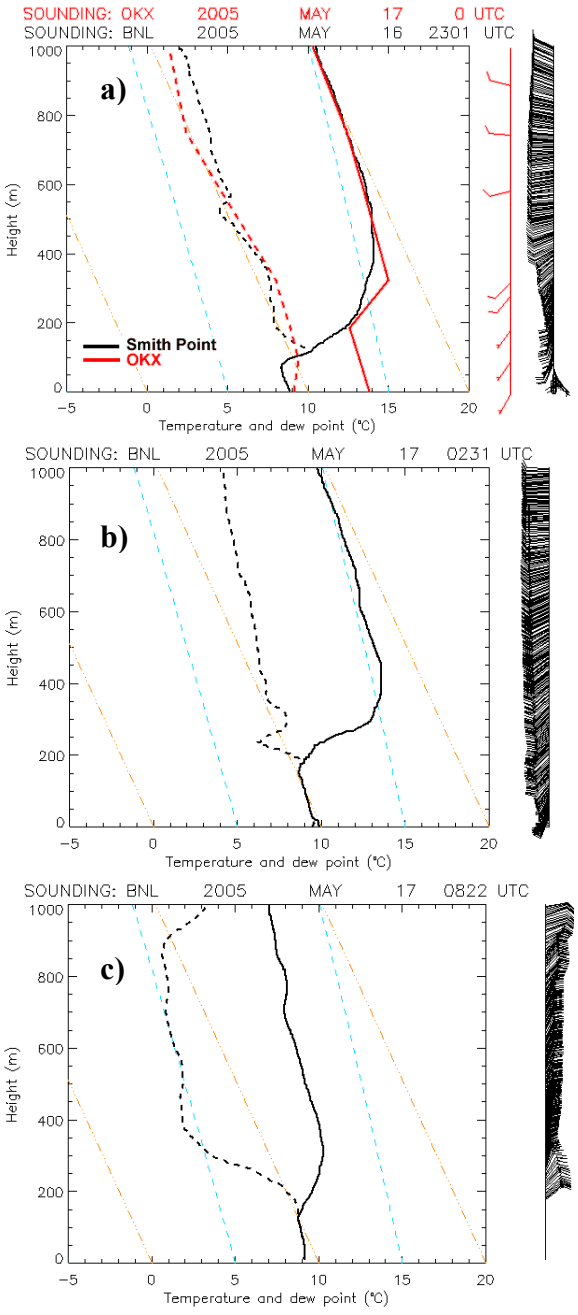

Figure 17. Profiles of temperature (solid line), dew point temperature (dashed line) and wind (barbs) at a) 23 UTC at OKX and Smith Point, b) 0231 UTC at BNL, c) 0822 UTC at BNL.

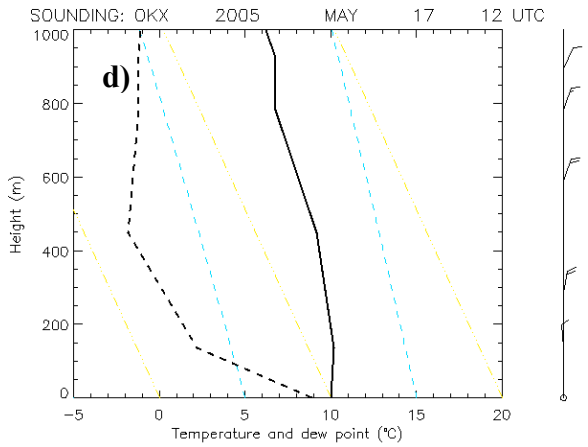

Figure 17 (continued). d) 12 UTC sounding at OKX (launched at ~11 UTC).

In terms of the dissipation of the cloud, an examination of the evolution of profiles from soundings launched between 0231 UTC and 12 UTC (Figs 17b to d) reveals a weakening cloud-top inversion along with a decrease in the moisture content of the lower atmosphere associated with a change in the wind direction. The 0822 UTC sounding, launched just before the complete dissipation of the low clouds, shows a drier layer between cloud top up to ~1000 m when compared to the earlier soundings. This layer corresponds to the depth over which the flow had turned to the N-NE. A comparison of specific humidity profiles from all available soundings shows a maximum decrease of 2.3 g kg^{-1} at 400 m during the period between 0231 UTC to 0822 UTC, with a delayed decrease in moisture at lower levels (Fig. 18). In fact, tower observations show only a slight decrease in specific humidity near the surface during the dissipation of the cloud layer (Fig. 19), suggesting that moisture advection was weak at lower levels. Interestingly, a decrease in surface moisture of the same magnitude as aloft is delayed until after 10 UTC, roughly 90 minutes after the dissipation of the low cloud layer.

Therefore it is suggested that the advection of drier air in a layer just above the cloud and its downward mixing were key factors in the dissipation of the cloud. A similar scenario was observed by Price (1999). Profiles from the 0822 UTC sounding are examined more closely to confirm this possible scenario. First, valid wind measurements from the sounding only begin at 150 m. The GPS tracking satellites did not lock on the sonde's signal for the first 40 seconds during the flight. Nevertheless, available measurements from the rawinsonde complemented with those from the instrumented tower show that the flow was between the NE to N in the lowest 1000 m, and the presence of a jet with a wind speed maximum of 13 m s^{-1} at 300 m (Fig. 20). Significant wind shear existed below the wind maxima. An assessment of the likelihood of turbulent motions within the inversion near cloud top is performed through the estimation of the bulk Richardson number for the layer between cloud top (130 m) and the top of the inversion (300 m). Values of virtual potential temperature and wind extracted from the available measurements are shown in Table II.

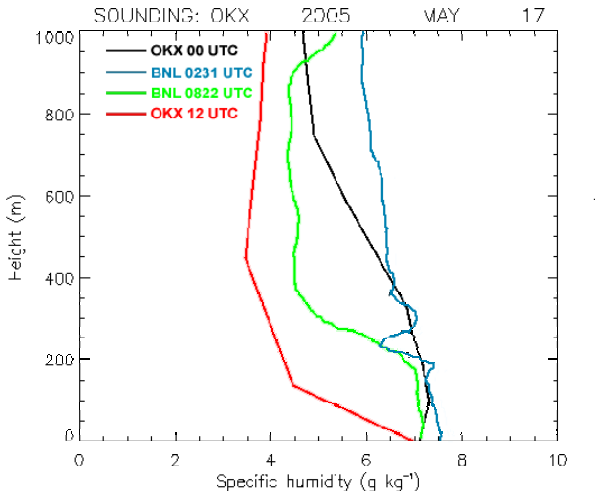

Figure 18. Profiles of specific humidity derived from rawinsonde measurements taken at or in the vicinity of the BNL tower site on the night and morning of May 17th 2005.

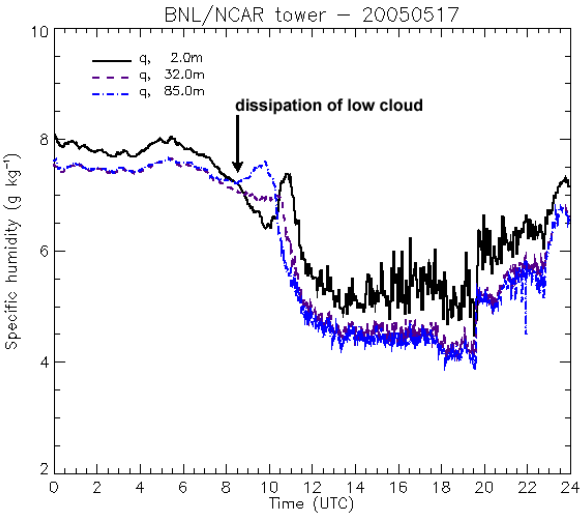

Figure 19. Temporal evolution of observed specific humidity at three levels on the BNL tower on May 17th 2005.

A value of $R_i \approx 0.16$ is found, smaller than the critical value of 0.25. This indicates the flow within the inversion just above cloud top was in all likelihood turbulent, allowing some downward mixing of the dry air within the cloud layer. Once again, the CTEI conditions are assessed using the available profiles. Using liquid water static energy and total water content values characterizing the well-mixed cloudy boundary layer and the atmosphere at the top of the capping inversion, $\Delta s_l \approx 4060$ J kg^{-1} and $\Delta q_t \approx -2.0$ g kg^{-1} are found,

yielding a value of $\kappa \approx 0.19$. A value of κ close to the critical value $\kappa_* = 0.23$ combined with a continuously decreasing moisture aloft suggest that the cloud layer was about to become unstable to the influence of cloud-top entrainment. Therefore, observations provide strong evidence that the rapid cloud dissipation that occurred shortly after the 0822 UTC sounding was indeed triggered by cloud-top entrainment of air from a layer where moisture was decreasing under the influence of horizontal advection in the northerly flow.

Table II. Values used in the computation of R_i, extracted from observed profiles at 0822 UTC May 17th 2005.

Height	θ_v (K)	Wind speed (m s^{-1})	Wind direction
130 m	283.4	5.5	54°
300 m	286.3	13.6	11°

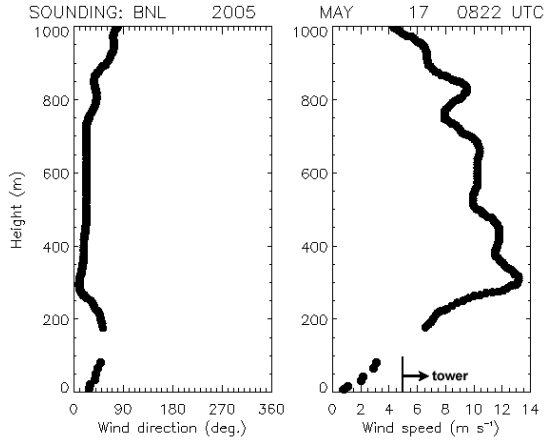

Figure 20. Profiles of wind direction and wind speed from the 0822 UTC rawinsonde and tower on May 17th 2005.

4. SUMMARY AND DISCUSSION

An analysis of conditions observed during low ceiling events was conducted, taking advantage of the availability of high-resolution profiles obtained from special soundings performed during an enhanced observing period at the FAA C&V instrumented site in May 2005. The availability of the high-resolution soundings proved to be critical in providing the information needed to gain an understanding of the mechanisms that influenced the life cycle of both low ceiling events.

Low ceiling events analyzed in this study were characterized by an unexpected intrusion of marine stratus inland in one case, while the other one was characterized by a rapid dissipation of a stratus cloud deck unrelated to the classical "burnoff" process. The results from the analysis of available data provided valuable insights into the mechanisms responsible for cloud propagation and persistence on the one hand, and cloud dissipation on the other. Key factors to the stratus intrusion were the evolving low level flow conditions associated with a coastal mesoscale circulation and the absence of a significant moisture contrast between the cloud layer and the lower free atmosphere above cloud top. The low level jet on the western edge of the coastal circulation provided for the advection of the cloudy air, while the absence of significant shear near cloud top minimized the influence of entrainment at cloud top. Even if significant entrainment was to occur, the water vapor content aloft was high enough to prevent cloud-top entrainment instability to occur. On the other hand, key factors to the rapid dissipation of a stratus cloud deck were the advection of drier air aloft and conditions conducive to the entrainment of the dry air across the cloud top interface.

These findings point toward the great difficulty of accurately forecasting such events. Stratiform cloud layers sensitively respond to combined influences from mesoscale and local scale processes, of which little information is readily available to weather forecasters. Mesoscale analyses and forecasts have arguably improved over the last few years, as evidenced here with the good correspondence between the RUC13 analyzed wind field offshore with the observed propagation of a marine stratus cloud. Although no effort has been undertaken to assess the performance of numerical weather forecast models with respect to the events discussed in this study, other studies have highlighted the shortcomings of some models at representing local scale processes, particularly with respect to boundary layer structure and stratiform clouds (Price and Bush 2004).

Furthermore, the absence of observations providing high spatial and temporal resolution information on the environment in which low clouds evolve does nothing to help forecasters with the production of very short-term C&V forecasts. In the cases illustrated in this study, accurate information about the evolving wind, temperature and moisture profiles in the vicinity of cloud top were found to be key elements toward a better understanding of the observed evolution of clouds and would also have arguably been key elements toward more accurate C&V nowcasts.

Another point of interest was the apparent decoupling between the evolving humidity conditions aloft and those observed at the surface in the case of the dissipation of the stratus layer. This suggests that relying on surface observations alone can lead to a source of error in the forecasting of cloud ceiling conditions. The importance of having information on the evolving structure of the atmosphere aloft is thus strongly suggested.

In conclusion, these results point toward the need to further our understanding of the mechanisms influencing the life cycle of low clouds and fog, and to perform targeted evaluations of the ability of numerical models at representing these mechanisms. From the point of view of input to forecast systems (data

assimilation with numerical models, predictors in statistical models and simply observations made available to forecasters), the need to better assess the performance of current remote sensing systems as well as developing new systems capable of providing high-resolution information about the evolution of wind, temperature and moisture in the boundary layer and in the lower free atmosphere is advocated, particularly for site-specific applications.

Acknowledgments

Mike Wyllie and Jeffrey Tongue are thanked for their help, as well as all the personnel of the aviation weather desk at the Upton NWS office for their cooperation. Thanks are extended to Mark Miller, R. Michael Reynolds and Victor A. Cassella of the Brookhaven National Laboratory, Earth Systems Science Division, for providing access to the tower facility and providing logistical support. Thanks are also due to Jeff Cole and Scott Landolt of NCAR/RAL for technical assistance before and during the EOP. This work was supported by the Federal Aviation Weather Research Program and is in response to requirements of the FAA. The views expressed are those of the author and do not necessarily represent the official policy of the U.S. government.

REFERENCES

Bankert, R. L. and J. D. Hawkins, 2004: Using supervised learning for specific meteorological satellite applications. Proceedings, *12th Conf. on Satellite Meteorology and Oceanography*, Amer. Meteor. Soc., Seattle WA.

Benjamin S. G., D. Dévényi, S. S. Weygandt, K. J. Brundage, J. M. Brown, G. A. Grell, D. Kim, B. E. Schwartz, T. G. Smirnova, T. L. Smith and G. S. Manikin, 2004: An hourly assimilation–forecast cycle: The RUC. *Mon. Wea. Rev.*, **132**, 495-518.

Clark, D. A., 2006 Terminal ceiling and visibility product development for northeast U.S. Airports. *This conference*.

Ellrod, G. P., 1995: Advances in the detection and analysis of fog at night using GOES multispectral infrared imagery. *Wea. Forecasting*, **10**, 606-619.

Herzegh, P. H., G. Wiener, R. L. Bankert, S. G. Benjamin, R. Bateman, J. Cowie, M. Tryhane and B. Weekley, 2006: Development of FAA national ceiling and visibility products: Challenges, strategies and progress. *This conference*.

Lock, A. P. and M. K. MacVean, 1999: The generation of turbulence and entrainment by buoyancy reversal. *Quart. J. Roy. Meteor. Soc.*, **125**, 1017-1038.

Moeng, C.-H., B. Stevens and P. P. Sullivan, 2005: Where is the interface of the stratocumulus-topped PBL?. *J. Atmos. Sci.*, **62**, 2626-2631.

Price, J. D., 1999: Observations of stratocumulus cloud break-up over land. *Quart. J. Roy. Meteor. Soc.*, **125**, 441-468.

—, and M. R. Bush, 2004: Comparisons between model forecast and observed boundary layer profiles and related comments on cloud prediction. *Wea. Forecasting*, **19**, 959-969.

Robasky, F. M. and F. W. Wilson, 2006: Statistical forecasting of northeast ceiling and visibility using standard weather observations. *This Conference*.

Siems S. T., C. S. Bretherton, M. B. Baker, S. Shy and R. E. Breidenthal, 1990: Buoyancy reversal and cloud-top entrainment instability. *Quart. J. Roy. Meteor. Soc.*, **116**, 705-739.

Stevens, B., D. H. Lenschow, I. Faloona, C.-H. Moeng, D. K. Lilly, B. Blomquist, G. Vali, T. Campos, H. Gerber, S. Haimov, B. Morley, and D. Thornton, 2003: On entrainment rates in nocturnal marine stratocumulus. *Quart. J. Roy. Meteor. Soc.*, **129**, 3469-3493.

Tardif, R., 2004: Characterizing fog occurrences in the Northeastern United States using historical data. *11th Conference on Aviation, Range and Aerospace Meteorology*, Amer. Meteor. Soc., Hyannis, MA.

—, J. A. Cole, P. H. Herzegh, S. D. Landolt, R. M. Rasmussen and M. L. Tryhane, 2004: First observations of fog and low ceiling environments at the FAA northeast ceiling and visibility field site. *11th Conference on Aviation, Range and Aerospace Meteorology*, Amer. Meteor. Soc., Hyannis, MA.

Ware, R., F. Solheim, R. Carpenter, J. Güeldner, J. Liljegren, T. Nehrkorn, F. Vandenberghe , 2003: A multi-channel radiometric profiler of temperature, humidity and cloud liquid. *Radio Sci.*, **38**(4), 8079, doi:10.1029/2002RS002856.